

Advancing Image Understanding in Poor Visibility Environments: A Collective Benchmark Study

Wenhan Yang*, Ye Yuan*, Wenqi Ren, Jiaying Liu, Walter J. Scheirer, Zhangyang Wang, Taiheng Zhang, Qiaoyong Zhong, Di Xie, Shiliang Pu, Yuqiang Zheng, Yanyun Qu, Yuhong Xie, Liang Chen, Zhonghao Li, and Chen Hong, Hao Jiang, Siyuan Yang, Yan Liu, Xiaochao Qu, Pengfei Wan, Shuai Zheng, Minhui Zhong, Taiyi Su, Lingzhi He, Yandong Guo, Yao Zhao, Zhenfeng Zhu, Jianning Chi, Huan Wang, Kai Wang, Yixiu Liu, Xingyu Gao, Zhenyu Chen, Yongzhou Li, Chang Guo, Jinxiu Liang, Jingwen Wang, Tianyi Chen, Yuhui Quan, Yong Xu, Bo Liu, Xin Liu, Qi Sun, Tingyu Lin, Xiaochuan Li, Feng Lu, Lin Gu, Shengdi Zhou, Cong Cao, Shizheng Wang, Ruizhe Liu, Jiangang Yang, Liguo Zhou, Likun Qin, Mingyue Feng

arXiv:1904.04474v3 [cs.CV] 5 Sep 2019

Abstract—Existing enhancement methods are empirically expected to help the high-level end computer vision task; however, that is observed to not always be the case in practice. We focus on object or face detection in poor visibility enhancements caused by bad weathers (haze, rain) and low light conditions. To provide a more thorough examination and fair comparison, we introduce three benchmark sets collected in real-world hazy, rainy, and low-light conditions, respectively, with annotated objects/faces. We launched the UG²⁺ challenge Track 2 competition in IEEE CVPR 2019, aiming to evoke a comprehensive discussion and exploration about whether and how low-level vision techniques can benefit the high-level automatic visual recognition in various scenarios. To our best knowledge, this is the first and currently largest effort of its kind. Baseline results by cascading existing enhancement and detection models are reported, indicating the highly challenging nature of our new data as well as the large room for further technical innovations. Thanks to a large participation from the research community, we are able to analyze representative team solutions, striving to better identify the strengths and limitations of existing mindsets as well as the future directions.

Index Terms—Poor visibility environment, object detection, face detection, haze, rain, low-light conditions

I. INTRODUCTION

Background. Many emerging applications, such as unmanned aerial vehicles (UAVs), autonomous/assisted driving, search and rescue robots, environment monitoring, security surveillance, transportation and inspection, hinge on computer vision-based sensing and understanding of outdoor environments [143]. Such systems concern a wide range of target tasks such as detection, recognition, segmentation, tracking, and parsing. However, the performance of visual sensing and understanding algorithms will be largely jeopardized by various challenging conditions in unconstrained and dynamic degraded environments, *e.g.*, moving platforms, bad weathers, and poor illumination. They can cause severe visual degradations such as reduced contrasts, detail occlusions, abnormal illumination, fainted surfaces and color shift.

While most current vision systems are designed to perform in clear environments, *i.e.*, where subjects are well observable without (significant) attenuation or alteration, a dependable

vision system must reckon with the entire spectrum of complex unconstrained outdoor environments. Taking autonomous driving as an example: the industry players have been tackling the challenges posed by inclement weathers; however, heavy rain, haze or snow will still obscure the vision of on-board cameras and create confusing reflections and glare, leaving the state-of-the-art self-driving cars in struggle (see a Forbes article). Another illustrative example can be found in city surveillance: even the commercialized cameras adopted by governments appear fragile in challenging weather conditions (see a news article). Therefore, it is highly desirable to study to what extent, and in what sense, such challenging visual conditions can be coped with, for the goal of achieving robust visual sensing and understanding in the wild, which benefits security/safety, autonomous driving, robotics, and an even broader range of signal and image processing applications.

A. Challenges and Bottlenecks

Despite the blooming research on removing or alleviating the impacts of those challenges, such as dehazing [9, 37, 54, 95], deraining [12, 16, 25, 26, 64, 80, 127, 133] and illumination enhancement [60, 79, 99, 105, 125], the current solutions see significant gaps from addressing the above-mentioned pressing real-world challenges. A collective effort for identifying and resolving those bottlenecks that they commonly face has also been absent.

One primary challenge arises from the **Data** aspect. Those challenging visual conditions usually give rise to nonlinear and data-dependent degradations that will be much more complicated than the well-studied noise or motion blur. The state-of-the-art deep learning methods are typically hungry for training data. The usage of synthetic training data has been prevailing, but may inevitably lead to domain shifts [77]. Fortunately, those degradations often follow some parameterized physical models. That will naturally motivate a combination of model-based and data-driven approaches. In addition to training, the lack of real-world test sets (and consequently, the usage of potentially oversimplified synthetic sets) have limited the practical scope of the developed algorithms.

The other main challenge is found in the **Goal** side. Most restoration or enhancement methods cast the handling of those

*The first two authors Wenhan Yang and Ye Yuan contributed equally.

Correspondence should be addressed to: Zhangyang Wang (atlaswang@tamu.edu), and Walter J. Scheirer (walter.scheirer@nd.edu)

challenging conditions as a post-processing step of signal restoration or enhancement after sensing, and then feed the restored data for visual understanding. The performance of high-level visual understanding tasks will thus largely depend on the quality of restoration or enhancement. Yet it remains questionable whether restoration-based approaches would actually boost the visual understanding performance, as the restoration/enhancement step is not optimized towards the target task and may bring in misleading information and artifacts too. For example, a recent line of researches [17, 54, 65, 68, 71, 72, 90, 102, 106, 112, 135] discuss on the intrinsic interplay relationship of low-level vision and high-level recognition/detection tasks, showing that their goals are not always aligned.

B. Overview of UG^{2+} Track 2

UG^{2+} Challenge Track 2 aims to evaluate and advance the robustness of object detection algorithms in specific poor-visibility situations, including challenging weather and lighting conditions. We structure Challenge 2 into three sub-challenges. Each challenge features a different poor-visibility outdoor condition, and diverse training protocols (paired versus unpaired images, annotated versus unannotated, *etc.*). For each sub-challenge, we collect a new benchmark dataset captured in realistic poor-visibility environments with real image artifacts caused by rain, haze, insufficiency of light:

- **Sub-Challenge 2.1: (Semi-)Supervised Object Detection in the Haze.** We provide 4,322 real-world hazy images collected from traffic surveillance, all labeled with object bounding boxes and categories (car, bus, bicycle, motorcycle, pedestrian), as the main training and/or validation sets. We also release another set of 4,807 unannotated real-world hazy images collected from the same sources (and containing the same classes of traffic objects, though not annotated), which might be used at the participants' discretion. There will be a held-out test set of 3,000 real-world hazy images, with the same classes of objects annotated.
- **Sub-Challenge 2.2: (Semi-)Supervised Face Detection in the Low Light Condition.** We provide 6,000 real-world low light images captured during the nighttime, at teaching buildings, streets, bridges, overpasses, parks *etc.*, all labeled with bounding boxes for human faces, as the main training and/or validation sets. We also provide 9,000 unlabeled low-light images collected from the same setting. Additionally, we provide a unique set of 789 paired low-light/normal-light images captured in controllable real lighting conditions (but unnecessarily containing faces), which can be used as parts of the training data at the participants' discretion. There will be a held-out test set of 4,000 low-light images, with human face bounding boxes annotated.
- **Sub-Challenge 2.3: Zero-Shot Object Detection with Raindrop Occlusions.** We provide 1,010 pairs of raindrop images and corresponding clean ground-truths (collected through physical simulations), as the training and/or validation sets. Different from Sub-Challenges 2.1

and 2.2, semantic annotations are unavailable on training/validation images. A held-out test set of 2,496 real-world raindrop images are collected from high-resolution driving videos, in diverse real scenes during multiple drives. We label bounding boxes for selected object categories: car, person, bus, bicycle, and motorcycle.

The ranking criteria will be the Mean average precision (mAP) on each held-out test set, with a default Intersection-of-Union (IoU) threshold as 0.5. If the ratio of the intersection of a detected region with an annotated object is greater than 0.5, a score of 1 is assigned to the detected region, and 0 otherwise. When mAPs with IoU as 0.5 are equal, the mAPs with higher IoUs (0.6, 0.7, 0.8) will be compared sequentially.

II. RELATED WORK

A. Datasets

Most datasets used for image enhancement/processing mainly targets at evaluating the quantitative (PSNR, SSIM, *etc.*) or qualitative (visual subjective quality) differences of enhanced images *w.r.t.* the ground truths. Some earlier classical datasets include Set5 [6], Set14 [131], and LIVE1 [104]. The numbers of their images are small. Subsequent datasets come with more diverse scene content, such as BSD500 [81] and Urban100 [39]. The popularity of deep learning methods has increased demand for training and testing data. Therefore, many newer and larger datasets are presented for image and video restoration, such as DIV2K [108] and MANGA109 [29] for image super-resolution, PolyU [123] and Darmstadt [89] for denoising, RawInDark [13] and LOL dataset [120] for low light enhancement, HazeRD [141], OHaze [3] and IHaze [2] for dehazing, Rain100L/H [127] and Rain800 [134] for rain streak removal, and RAINDROP [91] for raindrop removal. However, these datasets provide no integration with subsequent high-level tasks.

A few works [34, 103, 145] make preliminary attempts for event/action understanding, video summarization, or face recognition in unconstrained and potentially degraded environments. The following datasets are collected by aerial vehicles, including VIRAT Video Dataset [87] for event recognition, UAV123 [82] for UAV tracking, and a multi-purpose dataset [128]. In [83], an unconstrained Face Detection Dataset (UFDD) is proposed for face detection in adverse condition including weather-based degradations, motion blur, focus blur and several others, containing a total of 6,425 images with 10,897 face annotations. However, few works specifically consider the impacts of image enhancement and object detection/recognition jointly. Prior to this UG^{2+} effort, a number of latest works have taken the first stabs. A large-scale hazy image dataset and a comprehensive study – REalistic Single Image DEhazing (RESIDE) [56] – including paired synthetic data and unpaired real data is proposed to thoroughly examine visual reconstruction and vision recognition in hazy images. In [78], an Exclusively Dark (ExDARK) dataset is proposed with a collection of 7,363 images captured from very low-light environments with 12 object classes annotated on both image class level and local object bounding boxes. In [62], the authors present a new large-scale benchmark called

RESIDE and a comprehensive study and evaluation of existing single image deraining algorithms, ranging from full-reference metrics, to no-reference metrics, to subjective evaluation and the novel task-driven evaluation. Those datasets and studies shed new light on the comparisons and limitations of state-of-the-art algorithms, and suggest promising future directions. In this work, we follow the footsteps of predecessors to advance the fields by proposing new benchmarks.

B. Poor Visibility Enhancement

There are numerous algorithms aiming to enhance visibility of the degraded imagery, such as image and video denoising/inpainting [57, 73, 93, 116, 117], deblurring [96, 124], super-resolution [69, 70, 118, 119] and interpolation [130]. Here we focus on dehazing, low-light condition, and deraining, as in the UG²⁺ Track 2 scope.

Dehazing. Dehazing methods proposed in an early stage rely on the exploitation of natural image priors and depth statistics, *e.g.* locally constant constraints and decorrelation of the transmission [23], dark channel prior [37], color attenuation prior [144], nonlocal prior [5]. In [84, 142], Retinex theory is utilized to approximate the spectral properties of object surfaces by the ratio of the reflected light. Recently, Convolutional Neural Network (CNN)-based methods bring in the new prosperity for dehazing. Several methods [9, 95] rely on various CNNs to learn the transmission fully from data. Beyond estimating the haze related variables separately, successive works make their efforts to estimate them in a unified way. In [50, 86], the authors use a factorial Markov random field that integrates the estimation of transmission and atmosphere light. Some researchers focus on the more challenging night-time dehazing problem [63, 136]. In addition to image dehazing, AOD-Net [53, 54] considers the joint interplay effect of dehazing and object detection in an unified framework. The idea is further applied to video dehazing by extending the model into a light-weight video hazing framework [55]. In another recent work [98], the semantic prior is also injected to facilitate video dehazing.

Low Light Enhancement. All low-light enhancement methods can be categorized into three ways: hand-crafted methods, Retinex theory-based methods and data-driven methods. Hand-crafted methods explore and apply various image priors to single image low-light enhancement, *e.g.* histogram equalization [1, 88]. Some methods [59, 140] regard the inverted low-light images as hazy images, and enhance the visibility by applying dehazing. The retinex theory-based method [52] is designed to transform the signal components, reflectance and illumination, differently to simultaneously suppress the noise and preserve high-frequency details. Different ways [44, 45] are used to decompose the signal and diverse priors [27, 28, 35, 114] are applied to realize better light adjustment and noise suppression. Li *et al.* [60] further extended the traditional Retinex model to a robust one with an explicit noise term, and made the first attempt to estimate a noise map out of that model via an alternating direction minimization algorithm. A successive work [99] develops a fast sequential algorithm. Learning based low-light image enhancement methods [79, 105, 125] have also been studied, where low-light

images used for training are synthesized by applying random Gamma transformation on natural normal light images. Some recent works aim to build paired training data from real scenes. In [13], Chen *et al.* introduced a See-in-the-Dark (SID) dataset of short-exposure low-light raw images with corresponding long-exposure reference raw images. Cai *et al.* [10] built a dataset of under/over-contrast and normal-contrast encoded image pairs, in which the reference normal-contrast images are generated by Multi-Exposure image Fusion or High Dynamic Range algorithms. Recently, Jiang *et al.* [43] proposed for the first time an unsupervised generative adversarial network, that can be trained without low/normal-light image pairs, yet generalizing nicely and flexibly on various real-world images. **Deraining.** Single image deraining is a highly ill-posed problem. To address it, many models and priors are used to perform signal separation and texture classification. These models include sparse coding [46], generalized low rank model [16], nonlocal mean filter [48], discriminative sparse coding [80], Gaussian mixture model [64], rain direction prior [133], transformed low rank model [12]. The presence of deep learning has promoted the development of single image deraining. In [25, 26], deep networks take the image detail layer as their input. Yang *et al.* [127] proposed a deep joint rain detection and removal method to remove heavy rain streaks and accumulation. In [133], a novel density-aware multi-stream densely connected CNN is proposed for joint rain density estimation and removal. Video deraining can additionally make use of the temporal context and motion information. The early works formulate rain streaks with more flexible and intrinsic characteristics, including rain modeling [4, 7, 8, 16, 30–33, 42, 75, 101, 139]. The presence of learning-based method [14, 49, 61, 97, 110, 111, 121], with improved modeling capacity, brings new progress. The emergence of deep learning-based methods push performance of video deraining to a new level. Chen *et al.* [15] integrated superpixel segmentation alignment, and consistency among these segments and CNN-based detail compensation network into a unified framework. Liu *et al.* [74] presented a recurrent network integrating rain degradation classification, deraining and background reconstruction.

C. Visual Recognition under Adverse Conditions

A real-world visual detection/recognition system needs to handle a complex mixture of both low-quality and high-quality images. It is commonly observed that, mild degradations, *e.g.* small noises, scaling with small factors, lead to almost no change of recognition performance. However, once the degradation level passes a certain threshold, there will be an unneglected or even very significant effect on system performance. In [109], Torralba *et al.* showed that, there will be a significant performance drop in object and scene recognition when the image resolution is reduced to 32×32 pixels. In [146], the boundary where the face recognition performance is largely degraded is 16×16 pixels. Karahan *et al.* [47] found Gaussian noise with its standard deviation ranging from 10 to 20 will cause a rapid performance decline. In [22], more impacts of contrast, brightness, sharpness, and out-of-focus on face recognition are analyzed.

TABLE I
SUB-CHALLENGE 2.1: IMAGE AND OBJECT STATISTICS OF THE TRAINING/VALIDATION, AND THE HELD-OUT TEST SETS.

	#Images	#Bounding Boxes
Training/Validation	4,310	41,113
Test (held-out)	2,987	24,201

TABLE II

SUB-CHALLENGE 2.1: CLASS STATISTICS OF THE TRAINING/VALIDATION, AND THE HELD-OUT TEST SETS.

Categories	Car	Person	Bus	Bicycle	Motorcycle
RTTS	25,317	11,366	2,590	698	1,232
Test (held-out)	18,074	1,562	536	225	3,804

In the era of deep learning, some methods [19, 24, 126] attempt to first enhance the input image and then forward the output into a classifier. However, this separate consideration of enhancement may not benefit the successive recognition task, because the first stage may incur artifacts which will damage the second stage recognition. In [38, 146], class-specific features are extracted as a prior to be incorporated into the restoration model. In [135], Zhang *et al.* developed a joint image restoration and recognition method based on sparse representation prior, which constrains the identity of the test image and guides better reconstruction and recognition. In [54], Li *et al.* considered dehazing and object detection jointly. These two stage joint optimization methods achieve better performance than previous one-stage methods. In [68, 115], the joint optimization pipeline for low-resolution recognition is examined. In [71, 72], Liu *et al.* discussed the impact of denoising for semantic segmentation and advocated their mutual optimization. Lately, in [113], the algorithmic impact of enhancement algorithms for both visual quality and automatic object recognition is thoroughly examined, on a real image set with highly compound degradations. In our work, we take a further step to consider the joint enhancement and detection in bad weather environments. Three large-scale datasets are collected to inspire new ideas and novel methods in the related fields.

III. INTRODUCTION OF UG²⁺ TRACK 2 DATASETS

A. (Semi-)Supervised Object Detection in the Haze

In Sub-challenge 2.1, we use the 4,322 annotated real-world hazy images of the RESIDE RTTS set [56] as the training and/or validation sets (the split is up to the participants). Five categories of objects (car, bus, bicycle, motorcycle, pedestrian) are labeled with tight bounding boxes. We provide another 4,807 unannotated real-world hazy images collected from the same traffic camera sources, for the possible usage of semi-supervised training. The participants can optionally use pre-trained models (*e.g.*, on ImageNet or COCO), or external data. But if any pre-trained model, self-synthesized or self-collected data is used, that must be explicitly mentioned in their submissions, and the participants must ensure all their used data to be public available at the time of challenge submission, for reproduciblity purposes.

There is a held-out test set of 2,987 real-world hazy images, collected from the same sources, with the same classes of

TABLE III
SUB-CHALLENGE 2.2: COMPARISON OF LOW-LIGHT IMAGE UNDERSTANDING DATASETS.

Dataset	Training		Testing	
	#Image	#Face	#Image	#Face
ExDark	400	-	209	-
UFDD	-	-	612	-
DarkFace	6,000	43,849	4,000	37,711

objected annotated. Fig. 1 shows the basic statistics of the RTTS set and the held-out set. The held-out test set has a similar distribution of number of bounding boxes per image, bounding box size and relative scale of bounding boxes to input images compared to the RTTS set, but has relatively larger image size. Samples from RTTS set and held-out set can be found in Fig. 2 and Fig. 3.

B. (Semi-)Supervised Face Detection in the Low Light Condition

In Sub-challenge 2.2, we use our self-curated DARK FACE dataset. It is composed of 10,000 images (6,000 for training and validation, and 4,000 for testing) taken in under-exposure condition where human faces are annotated by human with bounding boxes; and 9,000 images taken with the same equipment in the similar environment without human annotations. Additionally, we provide a unique set of 789 paired low-light/normal-light images captured in controllable real lighting conditions (but unnecessarily containing faces), which can be optionally used as parts of the training data. The training and evaluation set includes 43,849 annotated faces and the held-out test set includes 37,711 annotated faces. Table III presents a summary of the dataset and Fig. 4 presents example images.

Collection and annotation. This collection consists of images recorded from Digital Single Lens Reflexes, specifically Sony α 6000 and α 7 E-mount cameras with different capturing parameters on several busy streets around Beijing, where faces of various scales and poses are captured. The images in this collection are open source content tagged with an Attribution-NonCommercial-NoDerivatives 4.0 International license¹. The resolution of these images is 1080×720 (down-sampled from $6K \times 4K$). After filtering out those without sufficient information (lacking faces, too dark to see anything, *etc.*), we select 10,000 images for human annotation. The bounding boxes are labeled for all the recognizable faces in our collection. We make the bounding boxes tightly around the forehead, chin, and cheek, using the LabelImg Toolbox². If a face is occluded, we only label the exposed skin region. If most of a face is occluded, we ignore it. For this collection, we observe commonly seen degradations in addition to under-exposure, such as intensive noise. The face number and resolution range distribution are displayed in Fig 6. Each annotated image contains 1-34 human faces. The face resolutions in these images range from 1×2 to 335×296 . The resolution of most faces in our dataset is below 300 pixel² and the the face number mostly falls into the range [1, 20].

¹<https://www.jet.org.za/clearinghouse/projects/primted/resources/creativecommons-licence>

²<https://github.com/tzutalin/labelImg>

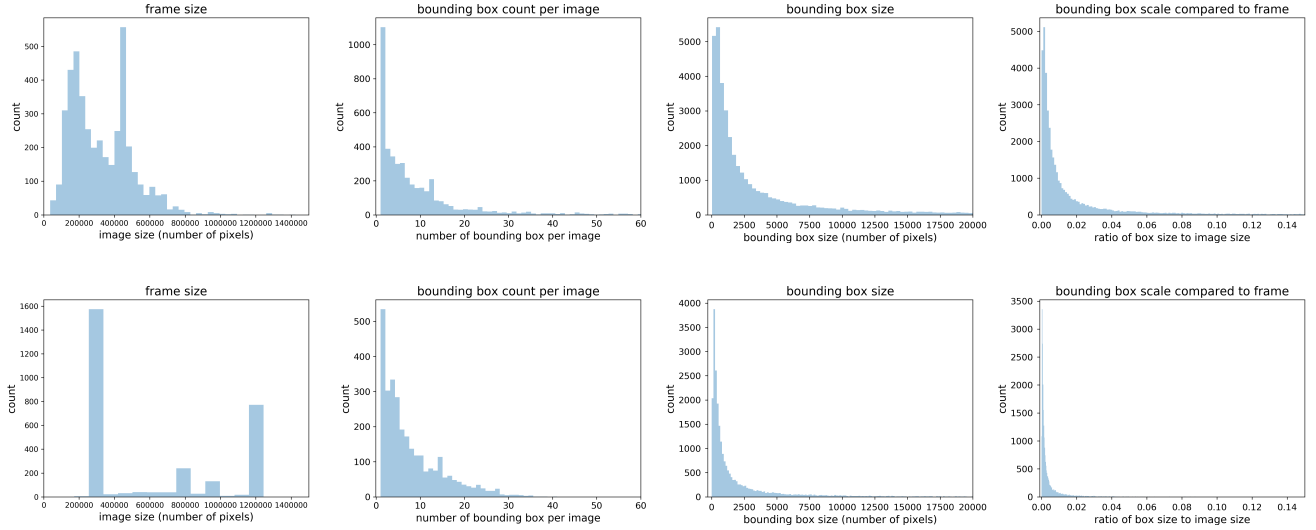


Fig. 1. Sub-challenge 2.1: Basic statistics on the training/validation set (the top row) and the held out test set (the bottom row). The first column shows the image size distribution (number of pixels per image), The second column the bounding box count distribution (number of bounding boxes per image), the third column the bounding box size distribution (number of pixels per bounding box), and the last column the ratios of bounding box size compared to frame size.



Fig. 2. Sub-challenge 2.1: Examples of images in training/validation set (i.e., RESIDE RTTS [56]).

TABLE IV
SUB-CHALLENGE 2.3: OBJECT STATISTICS IN THE HELD-OUT TEST SET.

Categories	Car	Person	Bus	Bicycle	Motorcycle
Test Set	7332	1135	613	268	968

C. Zero-Shot Object Detection with Raindrop Occlusions

In Sub-challenge 2.3, we release 1,010 pairs of realistic raindrop images and corresponding clean ground-truths, collected from the real scenes as described in [91], as the training and/or validation sets. Our held-out test set contains 2,495 real rainy images from high-resolution driving videos. As shown in Fig. 7, all images are contaminated by raindrops on camera lens. They are captured in diverse real traffic locations and scenes during multiple drives. We label bounding boxes for selected traffic objects: car, person, bus, bicycle, and motorcycle, which commonly appear on the roads of all



Fig. 3. Sub-challenge 2.1: Examples of images in the held-out test set.

images. Most images are of 1920×990 resolution, with a few exceptions of 4023×3024 resolution. The participants are free to use pre-trained models (e.g., ImageNet or COCO) or external data. But if any pre-trained model, self-synthesized or self-collected data is used, that must be explicitly mentioned in their submissions, and the participants must ensure their used data to be public available at the time of challenge submission, for reproducibility purposes.

IV. BASELINE RESULTS AND ANALYSIS

For all three sub-challenges, we report results by **cascading off-the-shelf enhancement methods and popular pre-**

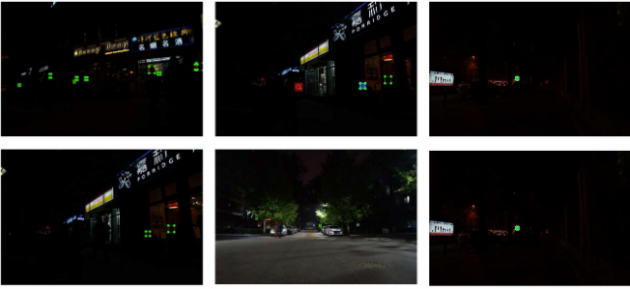


Fig. 4. Sub-challenge 2.2: Examples of images in DARK FACE collections.

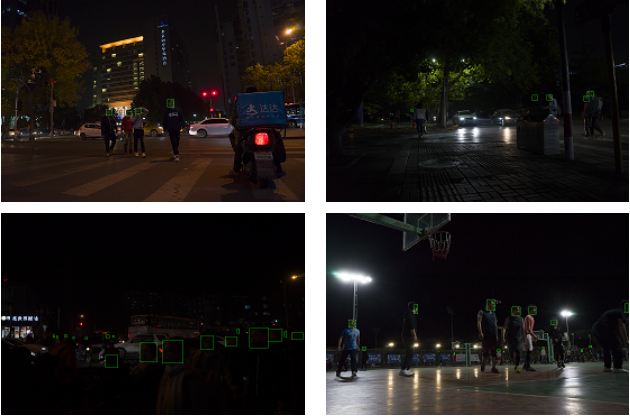


Fig. 5. Sub-challenge 2.2: DARK FACE has a high degree of variability in scale, pose, occlusion, appearance and illumination.

trained detectors. There has been no joint training performed, hence the baseline numbers are in no way very competitive. We expect to see much performance boosts over the baselines from the competition participants.

A. Sub-challenge 2.1 Baseline Results

1) *Baseline Composition:* We test four state-of-the-art object detectors: (1) **Mask R-CNN**³ [36]; (2) **RetinaNet**⁴ [67]; and (3) **YOLO-V3**⁵ [92]; (4) Feature Pyramid Network (**FPN**) [66]. We also try three state-of-the-art dehazing approaches: (a) **AOD-Net**⁷ [54]; (b) Multi-Scale Convolutional Neural Network (**MSCNN**)⁸ [95]; (c) Densely Connected Pyramid Dehazing Network (**DCPDN**)⁹ [132]. All dehazing models adopt officially released versions.

2) *Results and Analysis:* Fig. 8 shows the object detection performance on the original hazy images of RESIDE RTTS set using Mask R-CNN. The detectors are pretrained on Microsoft COCO, a large-scale object detection, segmentation, and captioning dataset. A more detailed detection performance on the five objects can be found in Table V. Results show that without preprocessing or dehazing, the object detectors

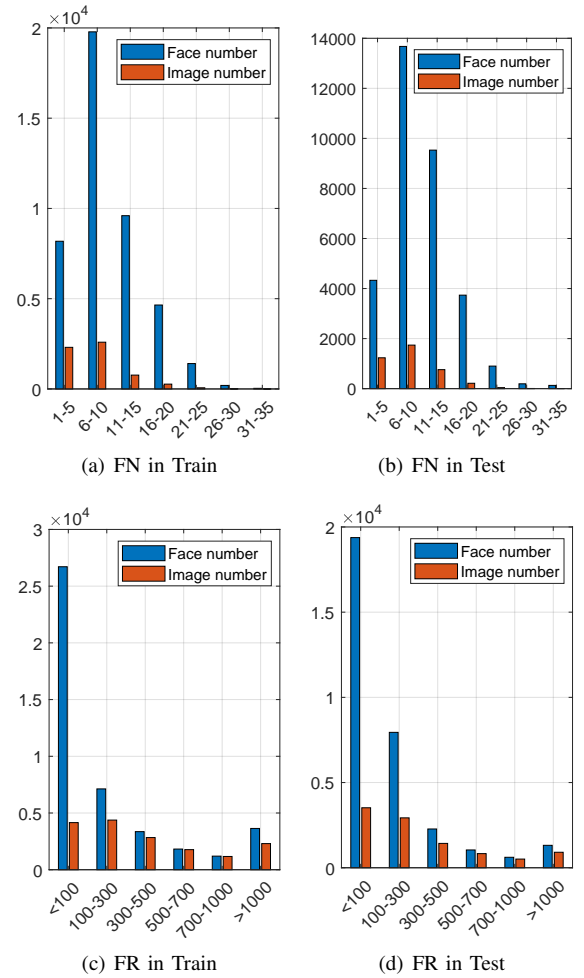


Fig. 6. Sub-challenge 2.2: Face resolution (FR) and face number (FN) distribution in DARK FACE collections. Image number denotes the number of images belonging to a certain category. Face number denotes the summation number of faces belonging to a certain category.

pretrained on clean images fail to predict a large amount of objects in the hazy image. The overall detection performance has a mAP of only 41.83% using Mask R-CNN and 42.54% using YOLO-V3. Among all the five object categories, person has the highest detection AP, while bus has the lowest AP.

We also compare the validation and test set performance in Table. V. One possible reason for the performance gap between validation and test sets is that the bounding box size of the latter is smaller compared to the former, as showed in Fig. 1 as well as visualized in Fig. 9.

3) *Effect of Dehazing:* We further evaluate the current state-of-the-art dehazing approaches on hazy dataset, with pre-trained detectors subsequently applied without tuning or adaptation. Fig. 9 shows two examples that dehazing algorithms can improve not only the visual quality of the images but also the detection accuracies. More detection results are included in Table. V. Detection mAPs of dehazed images using DCPDN and MSCNN approaches are 1% higher on average compared to those of hazy images.

Eventually, the choice of pre-trained detectors seem to also matter here: Mask R-CNN outperforms the other two detectors on both validation and test sets, before and after dehazing.

³https://github.com/matterport/Mask_RCNN

⁴<https://github.com/fizyr/keras-retinanet>

⁵<https://github.com/ayoooshkathuria/pytorch-yolo-v3>

⁶https://github.com/DetectionTeamUCAS/FPN_Tensorflow

⁷<https://github.com/Boyiliee/AOD-Net>

⁸<https://github.com/rwenqi/Multi-scale-CNN-Dehazing>

⁹<https://github.com/hezhangsprinter/DCPDN>

TABLE V
DETECTION RESULTS (mAP) ON THE RTTS (TRAIN/VALIDATION DATASET) AND HELD-OUT TEST SETS.

mAP			hazy	AOD-Net [54]	DCPDN [95]	MSCNN [132]
validation	* RetinaNet [67]	Person	55.85	54.93	56.70	58.07
		Car	41.19	37.61	42.68	42.77
		Bicycle	39.61	37.80	36.96	38.16
		Motorcycle	27.37	23.31	29.18	29.01
		Bus	16.88	15.70	16.34	18.34
		mAP	36.18	33.87	36.37	37.27
	* Mask R-CNN [36]	Person	67.52	66.71	67.18	69.23
		Car	48.93	47.76	52.37	51.93
		Bicycle	40.81	39.66	40.40	40.42
		Motorcycle	33.78	26.71	34.58	31.38
		Bus	18.11	16.91	18.25	18.42
	* YOLO-V3 [92]	mAP	41.83	39.55	42.56	42.28
		Person	60.81	60.21	60.42	61.56
		Car	47.84	47.32	48.17	49.75
		Bicycle	41.03	42.22	40.18	42.01
		Motorcycle	39.29	37.55	38.17	41.11
test	◊ FPN [66]	Bus	23.71	20.91	23.35	23.15
		mAP	42.54	41.64	42.06	43.52
		Person	51.85	52.35	51.04	54.50
		Car	37.48	36.05	37.19	38.88
		Bicycle	35.31	35.93	32.57	37.01
		Motorcycle	23.65	21.07	22.97	23.86
	RetinaNet	Bus	12.95	13.68	12.07	15.83
		mAP	32.25	31.82	31.17	34.02
		Person	17.64	18.23	16.65	19.34
		Car	31.41	29.30	33.31	32.97
		Bicycle	0.42	0.84	0.38	0.75
		Motorcycle	1.69	1.37	1.93	2.03
test	Mask R-CNN	Bus	12.77	13.70	12.07	15.82
		mAP	12.79	12.69	12.87	14.18
		Person	25.60	26.63	24.59	27.94
		Car	39.31	39.71	42.76	42.57
		Bicycle	0.64	0.52	0.22	0.37
		Motorcycle	3.37	2.81	2.83	2.99
	YOLO-V3	Bus	15.66	15.41	16.69	16.55
		mAP	16.92	17.02	17.42	18.09
		Person	20.64	21.41	21.42	22.11
		Car	34.68	33.90	34.52	35.93
		Bicycle	0.50	0.38	0.98	0.57
		Motorcycle	4.26	4.10	4.72	5.27
test	FPN	Bus	13.55	14.35	13.75	15.04
		mAP	14.69	14.83	15.08	15.78
		Person	12.65	12.57	11.13	14.19
		Car	30.54	31.24	27.81	32.68
		Bicycle	1.91	0.39	1.12	0.97
		Motorcycle	2.25	1.7	1.96	1.89
	DSFD	Bus	6.08	7.93	7.39	8.31
		mAP	10.69	10.77	9.88	11.61
		Person	12.65	12.57	11.13	14.19
		Car	30.54	31.24	27.81	32.68
		Bicycle	1.91	0.39	1.12	0.97
		Motorcycle	2.25	1.7	1.96	1.89

* RetinaNet, Mask R-CNN and YOLO-V3 are pretrained on Microsoft COCO dataset.

◊ FPN using ResNet-101 backbone is pretrained on the PASCAL Visual Object Classes (VOC) dataset.



Fig. 7. Sub-challenge 2.3: Example images from the held-out test set.

B. Sub-challenge 2.2 Baseline Results

1) **Baseline Composition:** We test four state-of-the-art deep face detectors: (1) Dual Shot Face Detector (**DSFD**) [58]¹⁰; (2) **Pyramidbox** [107]¹¹; (3) Single Stage Headless Face Detector (**SSH**) [85]¹²; (4) **Faster RCNN** [41]¹³.

We also include seven state-of-the-art algorithms for light/contrast enhancement: (a) Bio-Inspired Multi-Exposure Fusion (**BIMEF**) [129]¹⁴; (b) **Dehazing** [20]¹⁴; (c) Low-light Image Enhancement (**LIME**) [35]¹⁵; (d) **MF** [27]¹⁴; (e)

¹⁰<https://github.com/TencentYoutuResearch/FaceDetection-DSFD>

¹¹<https://github.com/EricZgw/PyramidBox>

¹²<https://github.com/mahyarnajibi/SSH.git>

¹³<https://github.com/playerkk/face-py-faster-rcnn>

¹⁴<https://github.com/baidut/BIMEF>

¹⁵<https://sites.google.com/view/xjguo/lime>

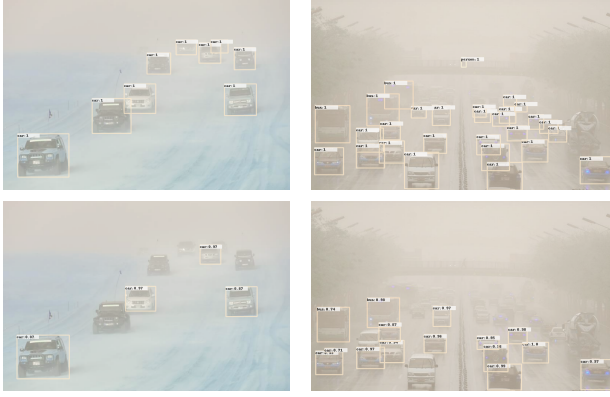


Fig. 8. Examples of object detection of hazy images on RESIDE RTTS set. The top row displays ground truth bounding boxes, the bottom row displays detected bounding boxes using pretrained Mask R-CNN.

Multi-Scale Retinex (**MSR**) [44]¹⁴; (f) Joint Enhancement and Denoising (**JED**) [99]¹⁶; (g) **RetinexNet** [120]¹⁷.

2) *Results and Analysis*: Fig. 12 (a) depicts the precision-recall curves of the original face detection methods, without enhancement. The baseline methods are trained on WIDER FACE [147]¹⁸, a large dataset with large scale variations in diversified factors and conditions. The results demonstrate that without proper pre-processing or adaptation, the state-of-the-art methods cannot achieve desirable detection rates on DARK FACE. Result examples are illustrated in Fig. 10. The evidences may imply that previous face datasets, though covering variations in poses, appearances, scale, *et al.*, are still insufficient to capture the facial features in the highly under-exposed condition.

3) *Effect of Enhancement*: We next use the enhancement algorithms to pre-process the annotated dataset and then apply the above two pre-trained face detection methods to the processed data. While the visual quality of the enhanced images is better, as expected, the detectors do perform better. As shown in Fig. 12 (b) and (c), in most instances, the precision of the detectors notably increases compared to that of the data without enhancement. Except for JED, various existing enhancement methods seem to result in similar improvements here. JED leads to only a small performance gain.

Despite being encouraging to see, the overall performance of the detectors still drops a lot compared to normal-light datasets. The simple cascade of low light enhancement and face detectors leave much improvement room open.

C. Sub-challenge 2.3 Baseline Results

1) *Baseline Composition*: We use four state-of-the-art object detection models: (1) Faster R-CNN (**FRCNN**) [94]; (2) **YOLO-V3** [92]; (3) **SSD-512** [76]; and (4) **RetinaNet** [67].

We employ five state-of-the-art deep learning-based deraining algorithms: (a) JOInt Rain DEtection and Removal¹⁹



Fig. 9. Examples of object detection of hazy images and dehazed images on RESIDE RTTS set. The first row displays the ground truth bounding boxes on hazy images, the second row displays detected bounding box on hazy image using pretrained Mask R-CNN, the bottom three columns displays Mask R-CNN detected bounding boxes on dehazed images using AOD-Net, MSCNN, DCPDN correspondingly.

(**JORDER**) [127]; (b) Deep Detail Network²⁰ (**DDN**) [26]; (c) Conditional Generative Adversarial Network²¹ (**CGAN**) [134]; (d) Density-aware Image De-raining method using a Multistream Dense Network²² (**DID-MDN**) [133]; and (e) **DeRaindrop**²³ [91]. For fair comparisons, we re-train all deraining algorithms using the same provided training set.

2) *Results and Analysis*: Table VI shows mAP results comparisons for different deraining algorithms using different detection models on the held-out test set. Unfortunately, we find that almost all existing deraining algorithms deteriorate the objects detection performance compared to directly using the rainy images for YOLO-V3, SSD-512, and RetinaNet (The only exception is the detection results by FRCNN). This could be due to those deraining algorithms are not trained towards the end goal of object detection, they are unnecessary to help this goal, and the deraining process itself might have lost discriminative, semantically meaningful true information, and thus hampers the detection performance. In addition, Table VI

¹⁶<https://github.com/tonghelen/JED-Method>

¹⁷<https://github.com/weichen582/RetinexNet>

¹⁸<http://shuoyang1213.me/WIDERFACE/>

¹⁹http://www.icsf.pku.edu.cn/struct/Projects/joint_rain_removal.html

²⁰https://github.com/XMU-smartdsp/Removing_Rain

²¹https://github.com/TrinhQuocNguyen/Edited_Original_IDCGAN

²²<https://github.com/hezhangsprinter/DID-MDN>

²³<https://github.com/rui1996/DeRaindrop>

shows that YOLO-V3 achieves the best detection performance, independent of deraining algorithms applied. We attribute this to the small objects in a relative long distance from the camera in the test set since YOLO-V3 is known to improve small object detection based on multi-scale prediction structure.

V. COMPETITION RESULTS: OVERVIEW & ANALYSIS

The UG²⁺ Challenge (Track 2) in conjunction with CVPR 2019 attracted large deals of attention and participation. More than 260 teams registered; among them, 82 teams finished the dry-run and submitted their final results successfully. Eventually, 6 teams were selected as winners (including a winner and a runner-up, for each sub-challenge).

In the following, we review a part of results from those participation teams who volunteer to disclose their technical details. The full leaderboards can be found at the website²⁴.

A. Sub-challenge 2.1: Competition Results and Analysis

A total of seven teams were able to outperform our best baseline numbers (mAP 18.09). The winner and runner-up teams, *HRI_DET* and *superlab403*, achieve record-high mAP results of 52.71 and 49.22, respectively. All teams used deep learning solutions. In addition to using most sophisticated networks, several interesting observations could be concluded: i) while many teams went with the dehazing-detection cascade idea (like our baselines, but usually jointly trained), the top-2 winners used end-to-end trained/adapted detection models on the hazy training set, without an (implicit) dehazing module; ii) the utilization of unlabeled data seems to open up much potential, and we believe it should be paid more attention to in future; and iii) multi-scale testing and ensembling contribute to many performance gains.

As the winner team, *HRI_DET* used Faster R-CNN, with the ImageNet-pretrained backbone of ResNeXt-101 [122] and Feature Pyramid Network (FPN) [66]. The Faster R-CNN was then tuned on the mixed dataset of MS COCO, PASCAL VOC and KITTI, with the common data augmentations. To further boost the performance, the team delved deep into the provided unlabeled hazy set, and adopted semi-supervised learning by using the unlabeled data to train the feature extractor with a reconstruction loss. The team used a batch size of 8 and trained the network using 8 Tesla M40 GPUs for 30,000 iterations with an initial learning rate of 0.005. They also found it helpful to apply stochastic weight averaging (SWA) [40] to aggregate several checkpoint models in one training pass, and further to ensemble multiple models (by averaging model weights) obtained from different training passes (*e.g.* with different learning rate schedulers). During inference, a three-scale testing is performed by resizing images to 1333×1000 , 1000×750 and 2100×600 . The third scale is applied to a closer view of the image, by cropping the foreground region defined as the bounding box of all high-confidence predictions with the first scale.

The runner-up team *superlab403* chose the Cascade R-CNN [11] baseline, and also replaced the original ResNet-101 backbone with ResNeXt-101. The team analyzed the

distribution of target aspect ratio from the training set, and selected four new anchor ratios (0.8, 1.7, 2.6, 3.7) by *k*-means. The team also did a (well-appreciated) label cleaning effort. Data augmentations such as blur, illumination change and color perturbations were adopted in training. The model was trained with an SGD optimizer; the initial learning rate was set as 0.0025, then being decayed by a factor of 0.1 at epochs 8, 11, 21 and 41 (total training epoch number 50).

Other teams have each developed their interesting solutions. For example, the *Mt. Star* team (ranked No. 3, mAP 31.24) adopted a sequential cascade of the dehazing model (DehazeNet [9]) and the detection model (Faster-RCNN), each first pre-trained on their own and then jointly tuned end-to-end on the training set. Multi-scale testing was adopted. The *ilab* team (ranked No. 6, mAP 19.15) also referred to the dehazing-detection cascade idea, but using DeblurGAN [51] (re-trained on haze data) for the dehazing model and Yolo-V2 [92] for the detection model, with a content loss.

B. Sub-challenge 2.2: Competition Results and Analysis

A total of three teams were able to outperform our best baseline numbers (mAP 41.40). The winner and runner-up teams, *CAS-Newcastle* and *CAS_NEU*, achieve high mAP results of 62.45 and 61.84, respectively. Similarly to Sub-challenge 2.1, all teams used deep learning solutions; yet interestingly, the most successful solutions are based on enhancement-detection cascades, showing a different trend with Sub-challenge 2.1.

The *CAS_NEU* team adopted a cascade of low-light enhancement (MSRCR [44]) and detection (RetinaNet [67]) models, where the detection model was directly trained on the enhancement model's preprocessed outputs. The *SCUT-CVC* team (ranked No. 7, mAP 35.18) found tone mapping [21] to be an impressively effective pre-processing, on top of which they tuned two DSFD detectors (with VGG-16 and ResNet-152 backbones), whose results were ensembled by late fusion. The *PHI-AI* team (ranked No. 7, mAP 29.95) adopted a U-Net [100] enhancer and a DSFD detector. The *tjfirst* team (ranked No. 12, mAP 26.50) referred to a more sophisticated enhancement module (first enhancing illumination by LIME [35], then super-resolving by DPSR [137], ended by denoising with BM3D [18]), followed by aggregating the DSFD-detection results on the original and enhanced images.

C. Sub-challenge 2.3: Competition Results and Analysis

Different from the first two sub-challenges, Sub-challenge 2.3 is substantially more difficult due to its “zero-shot” nature. Typical solutions that we see from the challenge teams include deraining + detection cascades; as well as ensembling multiple pre-trained detectors (*e.g.*, the *CAS-Newcastle-TUM* team). Unfortunately but not too surprisingly, none of the participation teams was able to outperform our baseline. That concurs with the conclusion drawn from the recent benchmark work [62]: *“Perhaps surprisingly at the first glance, we find that almost all existing deraining algorithms will deteriorate the detection performance compared to directly using the rainy images...”* *“No existing deraining method seems to directly help detection. That may encourage the community*

²⁴http://www.ug2challenge.org/leaderboard19_t2.html



Fig. 10. Sample face detection results of pretrained baseline on the original images of the proposed DARK FACE dataset.

to develop new robust algorithms to account for high-level vision problems on real-world rainy images. On the other hand, to realize the goal of robust detection in rain does not have to adopt a de-raining preprocessing; there are other domain adaptation type options...”. We expect to create a semi-supervised version of this challenge to alleviate the problem difficulty. Meanwhile, we also hope the results to remind the deraining community, of the possibly overlooked challenges of applying deraining to practice (when subsequent machine vision is the main goal).

VI. CONCLUSIONS

As concurred by most teams in the post-challenge feedbacks, it is widely agreed that the three sub-challenges in the UG²⁺ challenge 2019 Track 2 represent a very difficult, under-explored, yet high meaningful class of computer vision problems in practice. While some promising progress has been witnessed from the large volume of team participation, there remains large room to be improved. Through organizing this challenge, we expect to evoke a broader attention from the research community to address these challenges, which are barely covered by previous benchmarks. We look forward to making UG²⁺ a recurring event and also evolving/updating our problems and datasets every year.

REFERENCES

- [1] M. Abdullah-Al-Wadud, M. H. Kabir, M. A. A. Dewan, and O. Chae. A dynamic histogram equalization for image contrast enhancement. *IEEE Transactions on Consumer Electronics*, May 2007.
- [2] C. O. Ancuti, C. Ancuti, R. Timofte, and C. De Vleeschouwer. I-HAZE: a dehazing benchmark with real hazy and haze-free indoor images. *arXiv e-prints: 1804.05091*, April 2018.
- [3] C. O. Ancuti, C. Ancuti, R. Timofte, and C. De Vleeschouwer. O-HAZE: a dehazing benchmark with real hazy and haze-free outdoor images. *arXiv e-prints: 1804.05101*, April 2018.
- [4] P. C. Barnum, S. Narasimhan, and T. Kanade. Analysis of rain and snow in frequency space. *IJCV*, January 2010.
- [5] D. Berman, T. Treibitz, and S. Avidan. Non-local image dehazing. In *CVPR*, June 2016.
- [6] M. Bevilacqua, A. Roumy, C. Guillemot, and M. line Alberi Morel. Low-complexity single-image super-resolution based on nonnegative neighbor embedding. In *BMVC*, 2012.
- [7] J. Bossu, N. Hautière, and J.-P. Tarel. Rain or snow detection in image sequences through use of a histogram of orientation of streaks. *IJCV*, January 2011.
- [8] N. Brewer and N. Liu. Using the shape characteristics of rain to identify and remove rain from video. In *Joint IAPR International Workshops on SPR and SSPR*, 2008.
- [9] B. Cai, X. Xu, K. Jia, C. Qing, and D. Tao. Dehazenet: An end-to-end system for single image haze removal. *TIP*, November 2016.
- [10] J. Cai, S. Gu, and L. Zhang. Learning a deep single image contrast enhancer from multi-exposure images. *TIP*, April 2018.
- [11] Z. Cai and N. Vasconcelos. Cascade r-cnn: Delving into high quality object detection. In *CVPR*, pages 6154–6162, 2018.
- [12] Y. Chang, L. Yan, and S. Zhong. Transformed low-rank model for line pattern noise removal. In *ICCV*, Oct 2017.
- [13] C. Chen, Q. Chen, J. Xu, and V. Koltun. Learning to see in the dark. In *CVPR*, June 2018.
- [14] J. Chen and L. P. Chau. A rain pixel recovery algorithm for videos with highly dynamic scenes. *TIP*, March 2014.
- [15] J. Chen, C.-H. Tan, J. Hou, L.-P. Chau, and H. Li. Robust video content alignment and compensation for rain removal in a cnn framework. In *CVPR*.
- [16] Y.-L. Chen and C.-T. Hsu. A generalized low-rank appearance model for spatio-temporally correlated rain streaks. In *ICCV*, 2013.
- [17] B. Cheng, Z. Wang, Z. Zhang, Z. Li, D. Liu, J. Yang, S. Huang, and T. S. Huang. Robust emotion recognition from low quality and low bit rate video: A deep learning approach. In *IEEE International Conference on Affective Computing and Intelligent Interaction*, 2017.
- [18] K. Dabov, A. Foi, V. Katkovnik, and K. Egiazarian. Image denoising by sparse 3-d transform-domain collaborative filtering. *TIP*, Aug 2007.
- [19] C. Dong, Y. Deng, C. C. Loy, and X. Tang. Compression artifacts reduction by a deep convolutional network. In *ICCV*, 2015.
- [20] X. Dong, G. Wang, Y. Pang, W. Li, J. Wen, W. Meng, and Y. Lu. Fast efficient algorithm for enhancement of low lighting video. In *ICME*, 2011.
- [21] F. Drago, K. Myszkowski, T. Annen, and N. Chiba. Adaptive logarithmic mapping for displaying high contrast scenes. In *Computer Graphics Forum*, 2003.
- [22] A. Dutta, R. Veldhuis, and L. Spreeuwers. The impact of image quality on the performance of face recognition. In *Symposium on Information Theory in the Benelux and Joint WIC/IEEE Symposium on Information Theory and Signal Processing in the Benelux*, 2012.
- [23] R. Fattal. Single image dehazing. *TOG*, August 2008.
- [24] R. Fergus, B. Singh, A. Hertzmann, S. T. Roweis, and W. T. Freeman. Removing camera shake from a single photograph. In *TOG*, July 2006.
- [25] X. Fu, J. Huang, X. Ding, Y. Liao, and J. Paisley. Clearing the skies: A deep network architecture for single-image rain removal. *TIP*, June 2017.
- [26] X. Fu, J. Huang, D. Zeng, Y. Huang, X. Ding, and J. Paisley. Removing rain from single images via a deep detail network. In *CVPR*, 2017.
- [27] X. Fu, D. Zeng, Y. Huang, Y. Liao, X. Ding, and J. Paisley. A fusion-based enhancing method for weakly illuminated images. *Signal Processing*, 129:82 – 96, 2016.
- [28] X. Fu, D. Zeng, Y. Huang, X. P. Zhang, and X. Ding. In *CVPR*, June 2016.
- [29] A. Fujimoto, T. Ogawa, K. Yamamoto, Y. Matsui, T. Yamasaki, and K. Aizawa. Manga109 dataset and creation of metadata. In *Proc. of Int'l Workshop on coMics ANalysis, Processing and Understanding*, 2016.



Fig. 11. Sample face detection results of pretrained baseline on the enhanced images of the proposed DARK FACE dataset.

TABLE VI
DETECTION RESULTS (MAP) ON THE HELD-OUT TEST SET.

	Rainy	JORDER [127]	DDN [26]	CGAN [134]	DID-MDN [133]	DeRaindrop [91]
FRCNN [94]	16.52	16.97	18.36	23.42	16.11	15.58
YOLO-V3 [92]	27.84	26.72	26.20	23.75	24.62	24.96
SSD-512 [76]	17.71	17.06	16.93	16.71	16.70	16.69
RetinaNet [67]	23.92	21.71	21.60	19.28	20.08	19.73

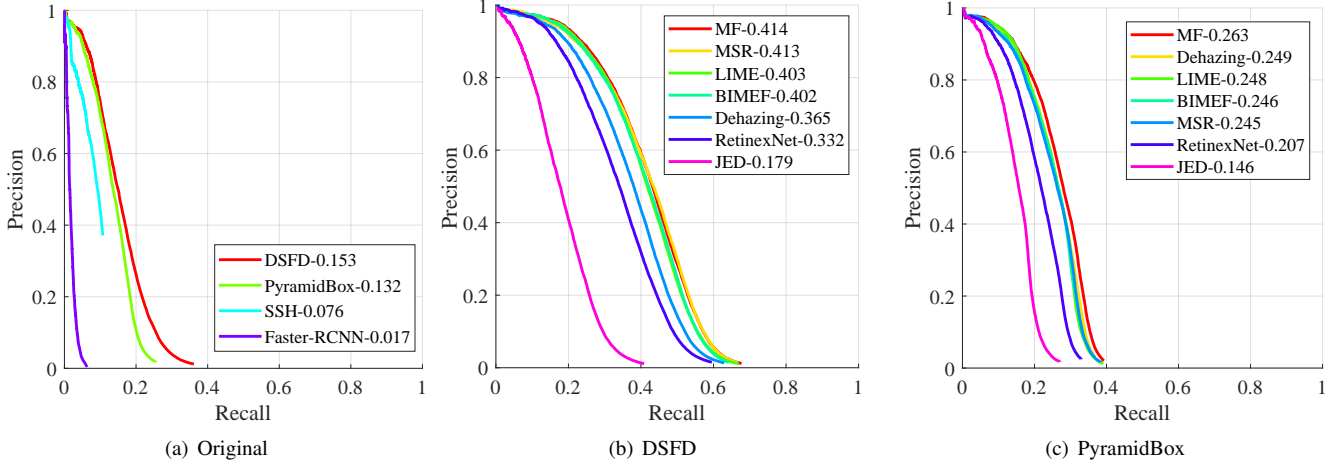


Fig. 12. Evaluation results of pretrained baseline on original and enhanced images of the proposed DARK FACE dataset.

- [30] K. Garg and S. K. Nayar. Detection and removal of rain from videos. In *CVPR*, 2004.
- [31] K. Garg and S. K. Nayar. When does a camera see rain? In *ICCV*, 2005.
- [32] K. Garg and S. K. Nayar. Photorealistic rendering of rain streaks. In *TOG*, August 2006.
- [33] K. Garg and S. K. Nayar. Vision and rain. *IJCV*, 2007.
- [34] M. Grgic, K. Delac, and S. Grgic. Sfface — surveillance cameras face database. *MTA*, February 2011.
- [35] X. Guo, Y. Li, and H. Ling. Lime: Low-light image enhancement via illumination map estimation. *TIP*, Feb 2017.
- [36] K. He, G. Gkioxari, P. Dollár, and R. Girshick. Mask r-cnn. In *CVPR*, 2017.
- [37] K. He, J. Sun, and X. Tang. Single image haze removal using dark channel prior. *TPAMI*, Dec 2011.
- [38] P. H. Hennings-Yeomans, S. Baker, and B. V. K. V. Kumar. In *CVPR*, 2008.
- [39] J. Huang, A. Singh, and N. Ahuja. Single image super-resolution from transformed self-exemplars. In *CVPR*, June 2015.
- [40] P. Izmailov, D. Podoprikhin, T. Garipov, D. Vetrov, and A. G. Wilson. Averaging weights leads to wider optima and better generalization. *arXiv preprint arXiv:1803.05407*, 2018.
- [41] H. Jiang and E. G. Learned-Miller. Face detection with the faster r-cnn. *IEEE Int'l Conf. on Automatic Face and Gesture Recognition*, 2017.
- [42] T.-X. Jiang, T.-Z. Huang, X.-L. Zhao, L.-J. Deng, and Y. Wang. A novel tensor-based video rain streaks removal approach via utilizing discriminatively intrinsic priors. In *CVPR*, July 2017.
- [43] Y. Jiang, X. Gong, D. Liu, Y. Cheng, C. Fang, X. Shen, J. Yang, P. Zhou, and Z. Wang. Enlightengan: Deep light enhancement without paired supervision. *arXiv preprint arXiv:1906.06972*, 2019.
- [44] D. J. Jobson, Z. Rahman, and G. A. Woodell. A multiscale retinex for bridging the gap between color images and the human observation of scenes. *TIP*, July 1997.
- [45] D. J. Jobson, Z. Rahman, and G. A. Woodell. Properties and performance of a center/surround retinex. *TIP*, Mar 1997.
- [46] L. W. Kang, C. W. Lin, and Y. H. Fu. Automatic single-image-based rain streaks removal via image decomposition. *TIP*, April 2012.
- [47] S. Karahan, M. Kilinc Yildirim, K. Kirtac, F. S. Rende, G. Butun, and H. K. Ekenel. How image degradations affect deep cnn-based face recognition? In *Int'l Conf. of the Biometrics Special Interest Group*, Sep. 2016.
- [48] J. H. Kim, C. Lee, J. Y. Sim, and C. S. Kim. Single-image deraining using an adaptive nonlocal means filter. In *ICIP*, 2013.
- [49] J. H. Kim, J. Y. Sim, and C. S. Kim. Video deraining and desnowing using temporal correlation and low-rank matrix completion. *TIP*, Sept 2015.
- [50] L. Kratz and K. Nishino. Factorizing scene albedo and depth from a single foggy image. In *ICCV*, 2009.
- [51] O. Kupyn, V. Budzan, M. Mykhailych, D. Mishkin, and J. Matas. Deblurgan: Blind motion deblurring using conditional adversarial networks. In *CVPR*, 2018.
- [52] E. H. Land. The retinex theory of color vision. *Sci. Amer.*, pages 108–128, 1977.
- [53] B. Li, X. Peng, Z. Wang, J. Xu, and D. Feng. An all-in-one network for dehazing and beyond. *arXiv preprint arXiv:1707.06543*, 2017.
- [54] B. Li, X. Peng, Z. Wang, J. Xu, and D. Feng. Aod-net: All-in-one dehazing network. In *ICCV*, 2017.
- [55] B. Li, X. Peng, Z. Wang, J. Xu, and D. Feng. End-to-end united video dehazing and detection. In *AAAI*, Feb. 2018.
- [56] B. Li, W. Ren, D. Fu, D. Tao, D. Feng, W. Zeng, and Z. Wang. Benchmarking single-image dehazing and beyond. *TIP*, 28(1):492–505, 2019.
- [57] H. Li, Z. Lu, Z. Wang, Q. Ling, and W. Li. Detection of blotch and scratch in video based on video decomposition. *TCSVT*, 23(11):1887–1900, 2013.
- [58] J. Li, Y. Wang, C. Wang, Y. Tai, J. Qian, J. Yang, C. Wang, J. Li, and F. Huang. Dsfd: Dual shot face detector. In *CVPR*.
- [59] L. Li, R. Wang, W. Wang, and W. Gao. A low-light image enhancement method for both denoising and contrast enlarging. In *ICIP*, 2015.
- [60] M. Li, J. Liu, W. Yang, X. Sun, and Z. Guo. Structure-revealing low-light image enhancement via robust retinex model. *TIP*, June 2018.
- [61] M. Li, Q. Xie, Q. Zhao, W. Wei, S. Gu, J. Tao, and D. Meng. Video rain streak removal by multiscale convolutional sparse coding. In *CVPR*, June 2018.
- [62] S. Li, I. B. Araujo, W. Ren, Z. Wang, E. K. Tokuda, R. H. Junior, R. Cesar-Junior, J. Zhang, X. Guo, and X. Cao. Single image deraining: A comprehensive benchmark analysis. *arXiv preprint arXiv:1903.08558*, 2019.
- [63] Y. Li, R. T. Tan, and M. S. Brown. Nighttime haze removal with glow and multiple light colors. In *ICCV*, Dec 2015.
- [64] Y. Li, R. T. Tan, X. Guo, J. Lu, and M. S. Brown. Rain streak removal using layer priors. In *CVPR*, 2016.
- [65] Y. li Tian. Evaluation of face resolution for expression analysis. In *CVPRW*, 2004.
- [66] T.-Y. Lin, P. Dollár, R. Girshick, K. He, B. Hariharan, and S. Belongie. Feature pyramid networks for object detection. In *CVPR*, 2017.

- [67] T.-Y. Lin, P. Goyal, R. Girshick, K. He, and P. Dollár. Focal loss for dense object detection. *TPAMI*, 2018.
- [68] D. Liu, B. Cheng, Z. Wang, H. Zhang, and T. S. Huang. Enhance visual recognition under adverse conditions via deep networks. *arXiv preprint arXiv:1712.07732*, 2017.
- [69] D. Liu, Z. Wang, Y. Fan, X. Liu, Z. Wang, S. Chang, and T. Huang. Robust video super-resolution with learned temporal dynamics. In *ICCV*, 2017.
- [70] D. Liu, Z. Wang, Y. Fan, X. Liu, Z. Wang, S. Chang, X. Wang, and T. S. Huang. Learning temporal dynamics for video super-resolution: A deep learning approach. *TIP*, March 2018.
- [71] D. Liu, B. Wen, J. Jiao, X. Liu, Z. Wang, and T. S. Huang. Connecting image denoising and high-level vision tasks via deep learning. *arXiv preprint arXiv:1809.01826*, 2018.
- [72] D. Liu, B. Wen, X. Liu, Z. Wang, and T. S. Huang. When image denoising meets high-level vision tasks: A deep learning approach. *arXiv preprint arXiv:1706.04284*, 2017.
- [73] J. Liu, S. Yang, Y. Fang, and Z. Guo. Structure-guided image inpainting using homography transformation. *TMM*, Dec. 2018.
- [74] J. Liu, W. Yang, S. Yang, and Z. Guo. Erase or fill? deep joint recurrent rain removal and reconstruction in videos. In *CVPR*, 2018.
- [75] P. Liu, J. Xu, J. Liu, and X. Tang. Pixel based temporal analysis using chromatic property for removing rain from videos. In *Computer and Information Science*, February 2009.
- [76] W. Liu, D. Anguelov, D. Erhan, C. Szegedy, S. Reed, C.-Y. Fu, and A. C. Berg. Ssd: Single shot multibox detector. In *ECCV*, 2016.
- [77] Y. Liu, G. Zhao, B. Gong, Y. Li, R. Raj, N. Goel, S. Kesav, S. Gottumukkala, Z. Wang, W. Ren, et al. Improved techniques for learning to dehaze and beyond: A collective study. *arXiv preprint arXiv:1807.00202*, 2018.
- [78] Y. P. Loh and C. S. Chan. Getting to know low-light images with the exclusively dark dataset. *CVIU*, January 2019.
- [79] K. G. Lore, A. Akintayo, and S. Sarkar. Llnet: A deep autoencoder approach to natural low-light image enhancement. *Pattern Recognition*, January 2017.
- [80] Y. Luo, Y. Xu, and H. Ji. Removing rain from a single image via discriminative sparse coding. In *ICCV*, 2015.
- [81] D. Martin, C. Fowlkes, D. Tal, and J. Malik. A database of human segmented natural images and its application to evaluating segmentation algorithms and measuring ecological statistics. In *ICCV*, 2001.
- [82] M. Mueller, N. Smith, and B. Ghanem. A benchmark and simulator for UAV tracking. In *ECCV*, 2018.
- [83] H. Nada, V. A. Sindagi, H. Zhang, and V. M. Patel. Pushing the Limits of Unconstrained Face Detection: a Challenge Dataset and Baseline Results. *arXiv e-prints*, page arXiv:1804.10275, Apr 2018.
- [84] D. Nair, P. A. Kumar, and P. Sankaran. An effective surround filter for image dehazing. In *Proc. of Int'l Conf. on Interdisciplinary Advances in Applied Computing*, 2014.
- [85] M. Najibi, P. Samangouei, R. Chellappa, and L. S. Davis. Ssh: Single stage headless face detector. In *ICCV*, 2017.
- [86] K. Nishino, L. Kratz, and S. Lombardi. Bayesian defogging. *IJCV*, July 2012.
- [87] S. Oh, A. Hoogs, A. Perera, N. Cuntoor, C. Chen, J. T. Lee, S. Mukherjee, J. K. Aggarwal, H. Lee, L. Davis, E. Squires, X. Wang, Q. Ji, K. Reddy, M. Shah, C. Vondrick, H. Pirsiavash, D. Ramanan, J. Yuen, A. Torralba, B. Song, A. Fong, A. Roy-Chowdhury, and M. Desai. A large-scale benchmark dataset for event recognition in surveillance video. In *CVPR 2011*, June 2011.
- [88] S. M. Pizer, R. E. Johnston, J. P. Ericksen, B. C. Yankaskas, and K. E. Muller. Contrast-limited adaptive histogram equalization: speed and effectiveness. In *Proceedings of Conference on Visualization in Biomedical Computing*, May 1990.
- [89] Tobias Plotz and S. Roth. Benchmarking Denoising Algorithms with Real Photographs. In *CVPR*, 2017.
- [90] R. Prabhu, X. Yu, Z. Wang, D. Liu, and A. Jiang. U-finger: Multi-scale dilated convolutional network for fingerprint image denoising and inpainting. *arXiv preprint arXiv:1807.10993*, 2018.
- [91] R. Qian, R. T. Tan, W. Yang, J. Su, and J. Liu. Attentive generative adversarial network for raindrop removal from a single image. In *CVPR*, 2018.
- [92] J. Redmon and A. Farhadi. Yolov3: An incremental improvement. *arXiv preprint arXiv:1804.02767*, 2018.
- [93] J. Ren, J. Liu, and Z. Guo. Context-aware sparse decomposition for image denoising and super-resolution. *TIP*, April 2013.
- [94] S. Ren, K. He, R. Girshick, and J. Sun. Faster r-cnn: Towards real-time object detection with region proposal networks. In *NIPS*, 2015.
- [95] W. Ren, S. Liu, H. Zhang, J. Pan, X. Cao, and M.-H. Yang. Single image dehazing via multi-scale convolutional neural networks. In *ECCV*, 2016.
- [96] W. Ren, J. Pan, X. Cao, and M.-H. Yang. Video deblurring via semantic segmentation and pixel-wise non-linear kernel. In *ICCV*, 2017.
- [97] W. Ren, J. Tian, Z. Han, A. Chan, and Y. Tang. Video desnowing and deraining based on matrix decomposition. In *CVPR*, 2017.
- [98] W. Ren, J. Zhang, X. Xu, L. Ma, X. Cao, G. Meng, and W. Liu. Deep video dehazing with semantic segmentation. *TIP*, April 2019.
- [99] X. Ren, M. Li, W.-H. Cheng, and J. Liu. Joint enhancement and denoising method via sequential decomposition. *ISCAS*, May 2018.
- [100] O. Ronneberger, P. Fischer, and T. Brox. U-net: Convolutional networks for biomedical image segmentation. In *International Conference on Medical image computing and computer-assisted intervention*, 2015.
- [101] V. Santhaseelan and V. K. Asari. Utilizing local phase information to remove rain from video. *IJCIV*, 112(1):71–89, March 2015.
- [102] C. Shan, S. Gong, and P. McOwan. Recognizing facial expressions at low resolution. In *Proc. of IEEE Conf. on Advanced Video and Signal Based Surveillance*, 2005.
- [103] J. Shao, C. C. Loy, and X. Wang. In *CVPR*, 2014.
- [104] H. R. Sheikh, M. F. Sabir, and A. C. Bovik. A statistical evaluation of recent full reference image quality assessment algorithms. *TIP*, Nov 2006.
- [105] L. Shen, Z. Yue, F. Feng, Q. Chen, S. Liu, and J. Ma. MSR-net: Low-light Image Enhancement Using Deep Convolutional Network. *ArXiv e-prints*, November 2017.
- [106] L. Stasiak, A. Pacut, and R. Vincente-Garcia. Face tracking and recognition in low quality video sequences with the use of particle filtering. In *Proc. of Annual Int'l Carnahan Conf. on Security Technology*, 2009.
- [107] X. Tang, D. K. Du, Z. He, and J. Liu. Pyramidbox: A context-assisted single shot face detector. In *ECCV*, 2018.
- [108] R. Timofte, E. Agustsson, L. Van Gool, M.-H. Yang, and L. Zhang. Ntire 2017 challenge on single image super-resolution: Methods and results. In *CVPRW*, 2017.
- [109] A. Torralba, R. Fergus, and W. T. Freeman. 80 million tiny images: A large data set for nonparametric object and scene recognition. *TPAMI*, November 2008.
- [110] A. K. Tripathi and S. Mukhopadhyay. A probabilistic approach for detection and removal of rain from videos. *IETE Journal of Research*, 57(1):82–91, 2011.
- [111] A. K. Tripathi and S. Mukhopadhyay. Video post processing: low-latency spatiotemporal approach for detection and removal of rain. *IET Image Processing*, 6(2):181–196, March 2012.
- [112] V. Vašek, V. Franc, and M. Urban. License plate recognition and super-resolution from low-resolution videos by convolutional neural networks. In *BMVC*, 2018.
- [113] R. G. VidalMata, S. Banerjee, B. RichardWebster, M. Albright, P. Davaulos, S. McCloskey, B. Miller, A. Tambo, S. Ghosh, S. Nagesh, et al. Bridging the gap between computational photography and visual recognition. *arXiv preprint arXiv:1901.09482*, 2019.
- [114] S. Wang, J. Zheng, H. M. Hu, and B. Li. Naturalness preserved enhancement algorithm for non-uniform illumination images. *TIP*, Sept 2013.
- [115] Z. Wang, S. Chang, Y. Yang, D. Liu, and T. S. Huang. Studying very low resolution recognition using deep networks. In *CVPR*, 2016.
- [116] Z. Wang, H. Li, Q. Ling, and W. Li. Robust temporal-spatial decomposition and its applications in video processing. *TCSVT*, March, 2013.
- [117] Z. Wang, D. Liu, S. Chang, Q. Ling, Y. Yang, and T. S. Huang. D3: Deep dual-domain based fast restoration of jpeg-compressed images. In *CVPR*, 2016.
- [118] Z. Wang, Y. Yang, Z. Wang, S. Chang, W. Han, J. Yang, and T. Huang. Self-tuned deep super resolution. In *CVPRW*, 2015.
- [119] Z. Wang, Y. Yang, Z. Wang, S. Chang, J. Yang, and T. S. Huang. Learning super-resolution jointly from external and internal examples. *TIP*, August 2015.
- [120] C. Wei, W. Wang, W. Yang, and J. Liu. Deep retinex decomposition for low-light enhancement. In *British Machine Vision Conference*, 2018.
- [121] W. Wei, L. Yi, Q. Xie, Q. Zhao, D. Meng, and Z. Xu. Should we encode rain streaks in video as deterministic or stochastic? In *ICCV*, 2017.
- [122] S. Xie, R. Girshick, P. Dollár, Z. Tu, and K. He. Aggregated residual transformations for deep neural networks. In *CVPR*, 2017.
- [123] J. Xu, H. Li, Z. Liang, D. Zhang, and L. Zhang. Real-world Noisy Image Denoising: A New Benchmark. *arXiv e-prints*, Apr 2018.
- [124] Y. Yan, W. Ren, Y. Guo, R. Wang, and X. Cao. Image deblurring via extreme channels prior. In *CVPR*, 2017.
- [125] J. Yang, X. Jiang, C. Pan, and C.-L. Liu. Enhancement of low light level images with coupled dictionary learning. In *ICCV*, 2016.
- [126] J. Yang, J. Wright, T. S. Huang, and Y. Ma. Image super-resolution via sparse representation. *TIP*, Nov 2010.
- [127] W. Yang, R. T. Tan, J. Feng, J. Liu, Z. Guo, and S. Yan. Deep joint rain detection and removal from a single image. In *CVPR*, 2017.

- [128] B. Z. Yao, X. Yang, and S.-C. Zhu. Introduction to a large-scale general purpose ground truth database: Methodology, annotation tool and benchmarks. In *EMMCVPR*, 2007.
- [129] Z. Ying, G. Li, and W. Gao. A Bio-Inspired Multi-Exposure Fusion Framework for Low-light Image Enhancement. *ArXiv e-prints*, November 2017.
- [130] Z. Yu, H. Li, Z. Wang, Z. Hu, and C. W. Chen. Multi-level video frame interpolation: Exploiting the interaction among different levels. *TCSVT*, January 2013.
- [131] R. Zeyde, M. Elad, and M. Protter. On single image scale-up using sparse-representations. In *Proc. of the Int'l Conf. on Curves and Surfaces*, pages 711–730, Berlin, Heidelberg, 2012.
- [132] H. Zhang and V. M. Patel. Densely connected pyramid dehazing network. In *CVPR*, 2018.
- [133] H. Zhang and V. M. Patel. Density-aware single image de-raining using a multi-stream dense network. In *CVPR*, 2018.
- [134] H. Zhang, V. Sindagi, and V. M. Patel. Image de-raining using a conditional generative adversarial network. *arXiv preprint arXiv:1701.05957*, 2017.
- [135] H. Zhang, J. Yang, Y. Zhang, N. M. Nasrabadi, and T. S. Huang. Close the loop: Joint blind image restoration and recognition with sparse representation prior. In *ICCV*, 2011.
- [136] J. Zhang, Y. Cao, S. Fang, Y. Kang, and C. W. Chen. In *CVPR*, 2017.
- [137] K. Zhang, W. Zuo, and L. Zhang. Deep plug-and-play super-resolution for arbitrary blur kernels. In *CVPR*, 2019.
- [138] S. Zhang, X. Zhu, Z. Lei, H. Shi, X. Wang, and S. Z. Li. S3fd: Single shot scale-invariant face detector. In *ICCV*, 2017.
- [139] X. Zhang, H. Li, Y. Qi, W. K. Leow, and T. K. Ng. Rain removal in video by combining temporal and chromatic properties. In *ICME*, 2006.
- [140] X. Zhang, P. Shen, L. Luo, L. Zhang, and J. Song. Enhancement and noise reduction of very low light level images. In *ICPR*, Nov 2012.
- [141] Y. Zhang, L. Ding, and G. Sharma. Hazerd: an outdoor scene dataset and benchmark for single image dehazing. In *ICIP*, 2017.
- [142] J. Zhou and F. Zhou. Single image dehazing motivated by retinex theory. In *Proc. of Int'l Symposium on Instrumentation and Measurement, Sensor Network and Automation*, pages 243–247, Dec 2013.
- [143] P. Zhu, L. Wen, D. Du, X. Bian, H. Ling, Q. Hu, Q. Nie, H. Cheng, C. Liu, X. Liu, et al. Visdrone-det2018: The vision meets drone object detection in image challenge results. In *ECCV*, 2018.
- [144] Q. Zhu, J. Mai, and L. Shao. A fast single image haze removal algorithm using color attenuation prior. *TIP*, Nov 2015.
- [145] X. Zhu, C. C. Loy, and S. Gong. Video synopsis by heterogeneous multi-source correlation. In *ICCV*, Dec 2013.
- [146] W. Zou and P. C. Yuen. Very low resolution face recognition problem. *TIP*, Jan 2012.
- [147] Shuo Yang, Ping Luo, Chen Change Loy, and Xiaou Tang. Wider face: A face detection benchmark. In *CVPR*, 2016.